



Research article

BMX deletion mitigates neuroinflammation induced by retinal ischemia/reperfusion through modulation of the AKT/ERK/STAT3 signaling cascade

Guangyi Huang^{a,1}, Shaoyang Zhang^{a,1}, Jing Liao^{a,1}, Yuanjun Qin^{a,1}, Yiyi Hong^{a,1}, Qi Chen^a, Yunru Lin^a, Yue Li^a, Lin Lan^a, Wen Hu^a, Kongqian Huang^a, Fen Tang^a, Ningning Tang^a, Li Jiang^a, Chaolan Shen^a, Ling Cui^a, Haibin Zhong^a, Min Li^a, Peng Lu^a, Qinmeng Shu^{b,**}, Yantao Wei^{c,***}, Fan Xu^{a,*}

^a Department of Ophthalmology, the People's Hospital of Guangxi Zhuang Autonomous Region & Guangxi Key Laboratory of Eye Health & Guangxi Health Commission Key Laboratory of Ophthalmology and Related Systemic Diseases Artificial Intelligence Screening Technology & Institute of Ophthalmic Diseases, Guangxi Academy of Medical Sciences, Nanning, 530021, Guangxi, China

^b Eye Institute, Eye and ENT Hospital, College of Medicine, Fudan University, Shanghai Key Laboratory of Visual Impairment and Restoration, Science and Technology Commission of Shanghai Municipality, Key Laboratory of Myopia (Fudan University), Chinese Academy of Medical Sciences, National Health Commission, Shanghai, China

^c State Key Laboratory of Ophthalmology, Zhongshan Ophthalmic Center, Sun Yat-sen University, Guangdong Provincial Key Laboratory of Ophthalmology and Visual Science, 7 Jinsui Road, Guangzhou, 510060, China

ARTICLE INFO

Keywords:

BMX
Apoptosis
Ischemia/reperfusion
Inflammation
Neuroprotection
Retina

ABSTRACT

Aims: Retinal ischemia/reperfusion (I/R) injury is implicated in the etiology of various ocular disorders. Prior research has demonstrated that bone marrow tyrosine kinase on chromosome X (BMX) contributes to the advancement of ischemic disease and inflammatory reactions. Consequently, the current investigation aims to evaluate BMX's impact on retinal I/R injury and clarify its implied mechanism of action.

Main methods: This study utilized male and female systemic BMX knockout (BMX^{-/-}) mice to conduct experiments. The utilization of Western blot assay and immunofluorescence labeling techniques was employed to investigate variations in the expression of protein and tissue localization. Histomorphological changes were observed through H&E staining and SD-OCT examination. Visual function changes were assessed through electrophysiological experiments. Furthermore, apoptosis in the retina was identified using the TUNEL assay, as well as the ELISA technique, which has been utilized to determine the inflammatory factors level.

Key findings: Our investigation results revealed that the knockdown of BMX did not yield a significant effect on mouse retina. In mice, BMX knockdown mitigated the negative impact of I/R injury on retinal tissue structure and visual function. BMX knockdown effectively reduced apoptosis, suppressed inflammatory responses, and decreased inflammatory factors subsequent to I/R injury. The outcomes of the current investigation revealed that BMX knockdown partially protected the retina through downregulating phosphorylation of AKT/ERK/STAT3 pathway.

* Corresponding authors.

** Corresponding author.

*** Corresponding author.

E-mail addresses: qshu12@fudan.edu.cn (Q. Shu), weiyantao75@126.com (Y. Wei), oph_fan@163.com (F. Xu).

¹ Contributed equally to the work.

<https://doi.org/10.1016/j.heliyon.2024.e27114>

Received 12 December 2023; Received in revised form 13 February 2024; Accepted 23 February 2024

Available online 24 February 2024

2405-8440/© 2024 Published by Elsevier Ltd.

This is an open access article under the CC BY-NC-ND license

(<http://creativecommons.org/licenses/by-nc-nd/4.0/>).

Significance: Our investigation showed that BMX^{-/-} reduces AKT, ERK, and STAT3 phosphorylation, reducing apoptosis and inflammation. Thus, this strategy protected the retina from structural and functional damage after I/R injury.

1. Introduction

Ischemia/reperfusion (I/R) involves restricting organ blood supply and then performing restoration of perfusion and reoxygenation. This phenomenon was documented across different tissues and organs throughout the body, including the liver, heart, kidneys, lungs, brain, and retina [1–4]. The retina, which is a crucial location for vision formation and it is the site of lesions that cause blinding eye disorders, has significant metabolic activity [5]. Several ischemic retinal disorders, such as ophthalmic artery occlusion, acute glaucoma, prematurity retinopathy, retinal vascular occlusion, and diabetic retinopathy, are caused by I/R injury of the retina. The aforementioned disorders have the potential to induce both structural and functional retinal deterioration, slow visual recovery, and lead to blindness.

Bone marrow tyrosine kinase on chromosome X (BMX) is a member of the Tec family of non-receptor tyrosine kinases, possessing Src homology (SH) 3 and SH2 structural domains, as well as carboxy-terminal kinase structural domains, which play critical roles in several biological processes, including cytokine signalling and inflammation [6–8]. Previous studies have shown that BMX is able to participate in the inflammatory response cascade by regulating Toll-like receptor-induced interleukin (IL)-6 production, while also interacting with Fas to induce IL-6 and tumor necrosis factor-alpha (TNF- α) production [9–11]. These observations suggest that BMX has the ability to trigger the release of downstream inflammatory factors. In addition, previous studies have demonstrated the activation of BMX in neuronal injury caused by H₂O₂ or ischemia, and it has been experimentally demonstrated that inhibiting BMX activity effectively mitigates neurodegeneration [12]. These findings strongly implicate BMX in the pathogenesis of ischemia diseases. Considering that inflammation and ischemia are important mechanisms in the progression of retinal I/R injury, we postulated that BMX may be critically involved in retinal I/R injury and may serve as a potential target for intervention.

Hence, the current investigation aimed to construct a retinal I/R model in animals to mimic the pathological progression of retinal ischemia-reperfusion. Subsequently, a sequence of investigations has been conducted to investigate the possible mitigating characteristics of BMX knockdown on retinal I/R injury and elucidate its implying mechanism.

2. Materials and methods

2.1. Animals and animal experiments

The current investigation used male and female BMX knockout (BMX^{-/-}) mice aged 6–8 weeks from Cyagen Biotechnology Co., Ltd., and C57BL/6 wild-type (WT) mice from Animal Experiment Center of Guangxi Medical University. The laboratory animals were housed in controlled conditions that were free from pathogens utilizing a barrier system, wherein a 12-h light and dark cycle was maintained. Additionally, the animals were fed with a standardized laboratory food source. The protocols implemented in the current investigation were in accordance with the standards specified in the ARVO Statement on the Use of Animals in Ophthalmic and Vision Research and the ARRIVE guidelines.

For the animal investigations within the current investigation, WT mice and BMX^{-/-} mice were subjected to random allocation into four distinct groups: (1) WT mice undergoing sham surgery (WT + sham) group, (2) WT mice undergoing I/R injury (WT + I/R) group, (3) BMX^{-/-} mice undergoing sham surgery (BMX^{-/-} + sham) group, and (4) BMX^{-/-} mice undergoing I/R injury (BMX^{-/-} + I/R) group.

2.2. I/R model

Retinal I/R injury has been stimulated following established protocols outlined in the previous study [13]. In summary, anesthesia was initially administered through intraperitoneal injection of a 1% pentobarbital solution, local anesthesia of the cornea was achieved using 0.5% bupivacaine hydrochloride, and the dilation of the pupil was accomplished using 0.5% tropicamide-phenylephrine eye drops. The anterior chamber of mouse underwent perfusion using a 32-gauge sterile needle attached to a suspended saline bag positioned 1.5 m above, ensuring a constant pressure of 110 mmHg for a duration of 1 h. During the perfusion, the observation of the disappearance of the retinal red reflex indicated the presence of retinal ischemia. Following the cessation of perfusion, the observation of restoration of the retinal red reflex indicated retinal reperfusion. Additionally, a sham surgery group was included, where the same surgical investigation was performed on the contralateral eye of mouse without elevating the saline bag.

2.3. Hematoxylin and eosin (H&E) staining

After meticulously enucleating and fixing the eyes, they were immersed in paraffin and sectioned. H&E staining was employed for the paraffin sections, and the resulting images were captured using a Panoramic MIDI scanner (3DHISTECH, Budapest, Hungary). To comprehensively analyze alterations in retinal histomorphometry, a sequence of images was acquired from multiple regions of the retina, specifically the central, middle, and peripheral areas, which were around 700, 2100, and 3500 μ m away from the optic disc,

consecutively [14]. The thickness of retinal structures in these specific regions was subsequently quantified utilizing ImageJ package supplied by the (NIH) in Bethesda, Maryland. The measured retinal structures encompassed the inner plexiform layer (IPL), ganglion cell layer (GCL), nerve fiber layer (NFL), inner nuclear layer (INL), outer plexiform layer (OPL), and outer nuclear layer (ONL).

2.4. Immunofluorescence

The retinal flat mount procedure commenced with the isolation of intact retinal tissue following the dissection of mice, which was subsequently treated with 4% paraformaldehyde (PFA) for a duration of 55 min. Subsequently, the tissue was permeabilized, blocked, and subjected to incubation overnight via primary antibodies (Supplementary Table 1) at 4 °C. On a subsequent day, the retinas underwent rinsing and incubation using the corresponding secondary antibodies for a duration of 2 h at normal temperature. The final step involved flattening the retina onto a microscope slide. To prepare retinal cryosections, intact mouse eyes were initially isolated and treated with 4% PFA overnight. Afterward, the eyes underwent a gradual dehydration process through immersion in sucrose solution. Finally, the eyes were immersed within the OCT compound and sliced at 10 µm. The resulting sections were then permeabilized, blocked, and subjected to overnight incubation with primary antibodies (Supplementary Table 1) at 4 °C. Afterward, the slices underwent incubation for 2 h using the corresponding secondary antibody on the following day.

Fluorescence images of the stained retinal flat mounts and retinal cryosections were obtained utilizing a Carl Zeiss laser scanning confocal microscope. The quantification of fluorescence signal in the images was conducted employing ImageJ package, constructed by (NIH) in Bethesda, Maryland.

2.5. TUNEL staining

The TUNEL staining kit (In Situ Cell Death Detection with Fluorescein; Roche) was employed for the detection of apoptosis in the retina-frozen sections. Before staining, the slices were fixed, permeabilized, and closed. Afterward, the slices underwent incubation using the TUNEL reagent mixture for 1 h at 37 °C, in accordance with the instructions for use. The retinal neurons were subsequently identified using β3-Tubulin markers and incubated with the corresponding secondary antibodies, while the nuclei underwent labeling via DAPI. Finally, photographs were obtained utilizing a laser scanning confocal microscope (Carl Zeiss).

2.6. High-resolution spectral domain optical coherence tomography (SD-OCT)

SD-OCT is commonly recognized as a non-invasive, in vivo method for examining retinal components [15]. In this study, the SPECTRALIS-OCT (Heidelberg, Germany) and a mouse objective lens were employed to explore the hierarchical organization of the mouse retina. Anesthesia and topical phenylephrine eye drops dilated the mice's pupils before imaging. Subsequently, the mice were positioned appropriately, and OCT scans were obtained in automatic real-time mode, with each scan possessing a quality index exceeding 28. Image J was employed to measure and evaluate the retinal nerve fiber layer (RNFL), ganglion cell complex (GCC), and the remaining structural thicknesses.

2.7. Electretinography (ERG)

For evaluating the functioning of retinal neurons in mice at specific time intervals, ERG was obtained as per established protocols. The mice were initially anesthetized and positioned on a self-heating platform. Pupil dilation was achieved using topiramate-phenylephrine drops, while sodium carboxymethylcellulose drops were applied to lubricate the cornea. ERG measurements were obtained using a gold-plated wire ring electrode in direct contact with the corneal surface, serving as the active electrode. In preparation for scotopic ERG testing, mice were subjected to a minimum of 12 h of dark adaptation. The response amplitudes were subsequently quantified at three progressively elevating amounts of 0.01, 3.0, and 10.0 cd s m⁻². The photopic negative response (PhNR) has been elicited by a flash stimulus with an amount of 3.0 cd s m⁻², generated by a white light system, and the response amplitude was recorded using the Celeris Diagnostics system.

2.8. ELISA

The concentrations of inflammatory cytokines in the supernatants of retinal homogenates were assessed by employing ELISA kits (eBioscience, San Diego, CA, USA). The manufacturer's guidelines were strictly followed to execute the specific experimental procedures. Initially, the ELISA 96-well plate was coated with a capture antibody and subsequently sealed with a BSA-blocking solution. The plate was then washed thrice with PBS, following which 100 µL of diluted retinal supernatant samples or standards were introduced into the ELISA well plate. Subsequently, a membrane was placed over the plate and underwent incubation for 90 min at 37 °C. Subsequently, the liquid was disposed of and subjected to dehydration. Following this, 100 µL of a detection working solution has been supplemented to each well. The plate was then lined and underwent incubation at a temperature of 37 °C for 1 h. A volume of 100 µL of HRP conjugate working solution was introduced to every well after three PBS washes. The plate was then lined and subjected to incubation at a temperature of 37 °C for 30 min. Dispose of the liquid within the wells and wash the plate five times. Subsequently, 90 µL of substrate solution was introduced into every well, and the plate was subjected to incubation with the membrane at 37 °C for 15 min away from light. Following this, a 50 µL volume of termination solution was supplemented to every well to halt the reaction, resulting in a transformation of the blue color to yellow. Promptly following the investigation, the enzyme-linked equipment was

utilized to determine every well's optical density at 450 nm.

2.9. Western blot

Total proteins were extracted from the retinas of each group of mice using RIPA protein lysis solution. The resulting protein samples underwent SDS-PAGE protein separation, membrane transfer, and sealing. The PVDF membrane was then subjected to primary antibody immersion (dilution concentration: 1:1000, Supplementary Table 1), gentle shaking on a shaking table, and overnight incubation at 4 °C. Following this, the PVDF membrane was subjected to three 5-min washes with TBST. For secondary antibody incubation, the PVDF membrane was immersed in the secondary antibody (dilution: 1:5000), gently shaken on a shaking table, and incubated at normal temperature. ChemiDoc touch imaging system (Bio-Rad, Richmond, CA, USA) was utilized for protein identification, followed by Image Lab version 6.0 package (Bio-Rad) for quantification of protein intensity.

2.10. Statistical analysis

The investigations were performed three times, with independent repetitions, and the resulting information was quantified and

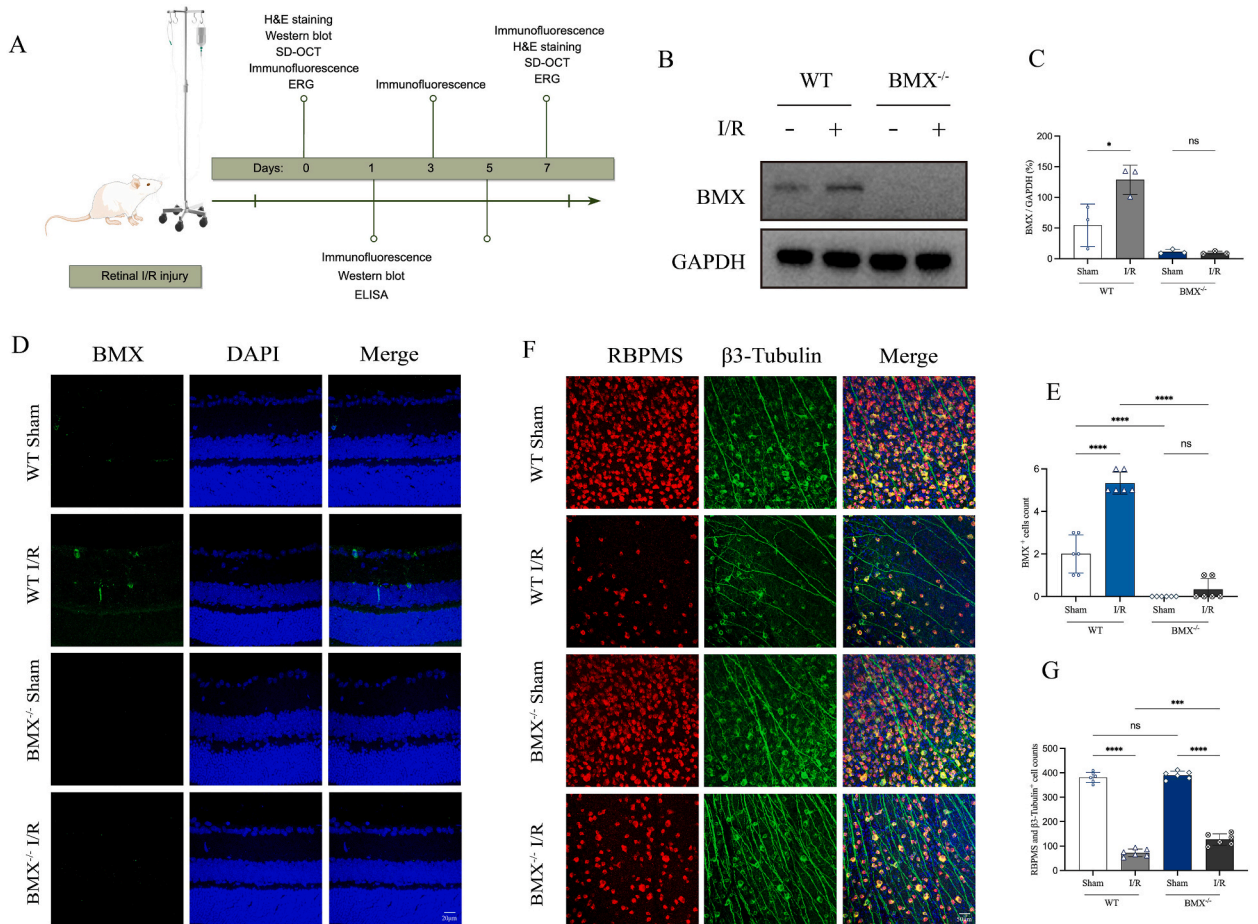


Fig. 1. BMX expression level has been elevated within the retinal I/R model, and BMX^{-/-} prevented RGCs loss after I/R injury. (A) The overall flowchart of the experimental plan by Figdraw. (B–C) Western blot and densitometry analyses of BMX expression in WT + sham group, WT + I/R group, BMX^{-/-} + sham group, and BMX^{-/-} + I/R group, respectively, with GAPDH utilized as a loading control. n = 3. (D) Representative immunofluorescence images of BMX (green) and DAPI (blue) in WT + sham group, WT + I/R group, BMX^{-/-} + sham group, and BMX^{-/-} + I/R group, respectively. Scale bars = 20 μm. (E) Measurement of the BMX fluorescence intensity. n = 6. (F) Representative immunofluorescence images of RBPMS (red), β-Tubulin (green), and DAPI (blue) in WT + sham group, WT + I/R group, BMX^{-/-} + sham group, and BMX^{-/-} + I/R group, respectively. Scale bars = 50 μm. (G) Measurement of RBPMS- and β-Tubulin-positive retinal ganglion cells. n = 6. Data are presented as mean ± SEM, and statistical significance has been identified employing One-way ANOVA subsequent by Tukey's Honest Significant Difference test. BMX, Bone marrow tyrosine kinase on chromosome X; I/R, ischemia/reperfusion; WT, wild type; ns, nonsignificant; In this context, the symbols *, **, ***, and **** correspond to P-values that are below the thresholds of 0.05, 0.01, 0.001, and 0.0001, respectively. (For interpretation of the references to color in this figure legend, the reader is referred to the Web version of this article.)

statistically analyzed by two researchers who were blinded to the study. The data have been expressed as mean ± standard deviation (SD), and group comparative analysis was conducted utilizing one-way ANOVA or Tukey’s honest significant variation test. Statistical analysis and data presentation were carried out utilizing GraphPad Prism (version 9.5.0, GraphPad Software, CA, USA), and statistical significance was considered *P* values less than 0.05.

3. Result

3.1. Increased BMX expression in the I/R model Retina

In order to examine potential alterations in BMX expression levels in the I/R model, we compared the protein levels of BMX in mice retinas from the WT + I/R group and the WT + sham group. The retinas of I/R mice reveal a significant upregulation for BMX protein

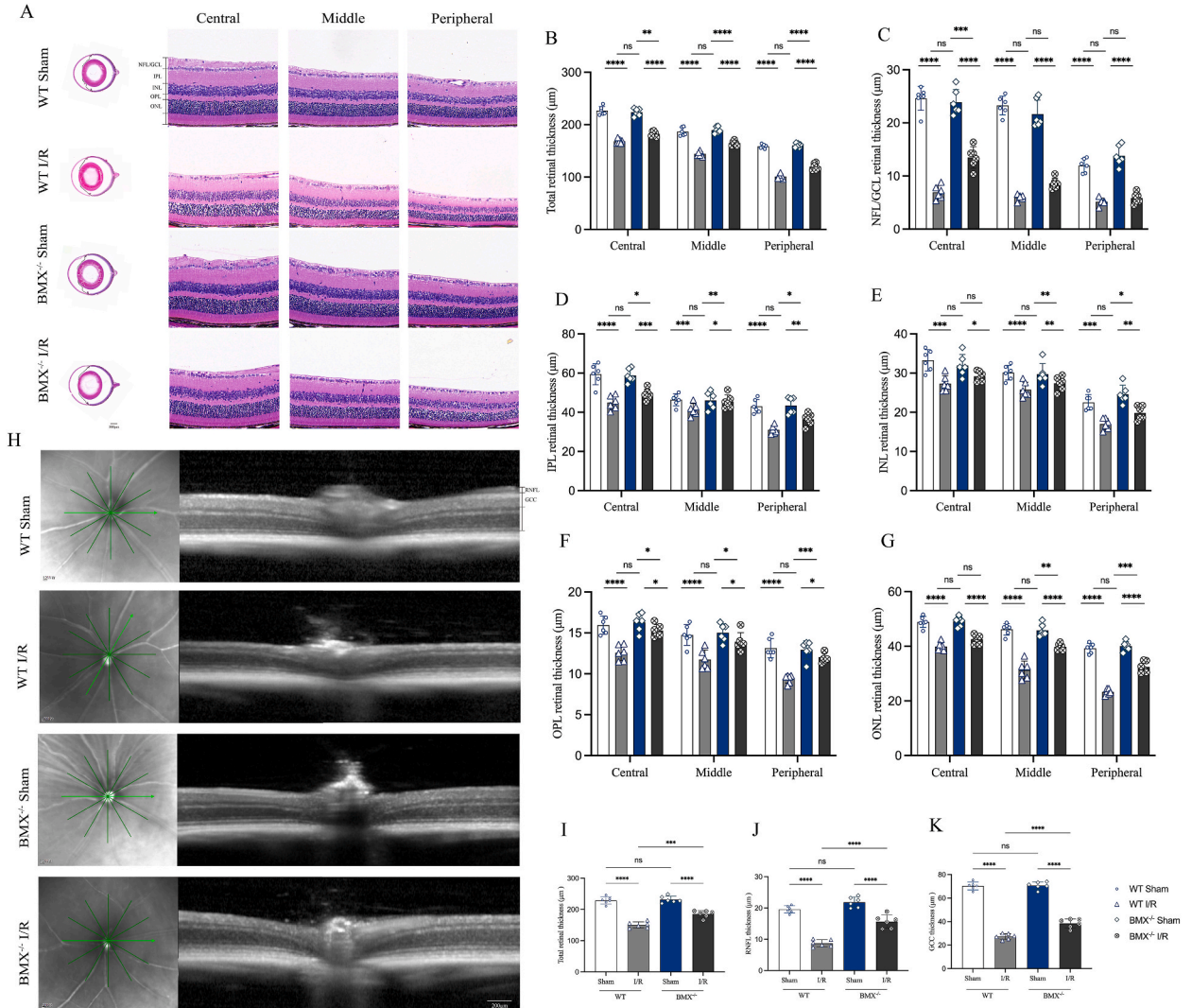


Fig. 2. BMX^{-/-} ameliorated damage to retinal structures after I/R injury. (A) Representative H&E staining images of the central, middle, and peripheral retina in WT + sham group, WT + I/R group, BMX^{-/-} + sham group, and BMX^{-/-} + I/R group, respectively. Scale bars = 20 µm. (B–G) Measurement of the total retina thickness, NFL/GCL, IPL, INL, OPL, and ONL of the retina. *n* = 6. (H) Representative SD-OCT images of the retina in WT + sham group, WT + I/R group, BMX^{-/-} + sham group, and BMX^{-/-} + I/R group, respectively. Scale bars = 200 µm. (I–K) Measurement of the total retina thickness, RNFL, and GCC of the retina. *n* = 6. Data are expressed as mean ± SEM and statistical significance has been identified utilizing One-way ANOVA subsequent by Tukey’s Honest Significant Difference test. BMX, Bone marrow tyrosine kinase on chromosome X; I/R, ischemia/reperfusion; WT, wild type; H&E, hematoxylin, and eosin; NFL, nerve fiber layer; GCL, ganglion cell layer; IPL, inner plexiform layer; INL, inner nuclear layer; OPL, outer plexiform layer; ONL, outer nuclear layer; SD-OCT, spectral domain optical coherence tomography; RNFL, retinal nerve fiber layer; GCC, ganglion cell complex, involving RNFL, GCL, and IPL; ns, nonsignificant; In this context, the symbols *, **, ***, and **** correspond to *P*-values that are below the thresholds of 0.05, 0.01, 0.001, and 0.0001, respectively.

levels, according to Western blot analysis (Fig. 1B and C). Furthermore, the immunofluorescence staining analysis revealed significant overexpression of BMX expression within the I/R group retinas, with a predominant concentration in the inner retina (Fig. 1D and E). Throughout the current investigation, we propose the hypothesis that retinal I/R injury in mice is linked to an increased presence of BMX.

To further substantiate the involvement of BMX within retinal I/R injury, we used $BMX^{-/-}$ mice for subsequent experimental investigations. The successful knockout of BMX was verified by Western blot analysis (Fig. 1B and C) and immunofluorescence staining of retinal sections (Fig. 1D and E).

3.2. $BMX^{-/-}$ prevented RGCs loss following I/R injury

RGCs, a crucial retinal constituent, exhibit converging axons that form the optic nerve and perform a crucial function within the transmission of visual information. In order to evaluate the extent of damage and survival of RGCs subsequent to I/R injury, we conducted immunofluorescence analysis utilizing RBPMS and β 3-Tubulin, which serve as specific markers for RGCs across the entire retina. Our findings indicated a noteworthy reduction in the quantity of retinal RBPMS- and β 3-Tubulin-positive cells in WT mice seven days' duration following I/R injury, contrasted with $BMX^{-/-}$ mice, where the number of retinal RBPMS- and β 3-Tubulin-positive cells was observed to be higher (Fig. 1F and G). These findings imply that $BMX^{-/-}$ provides partial relief from the damage of retinal RGCs stimulated via I/R and that BMX contributes to the demise of retinal RGCs following I/R to a certain degree.

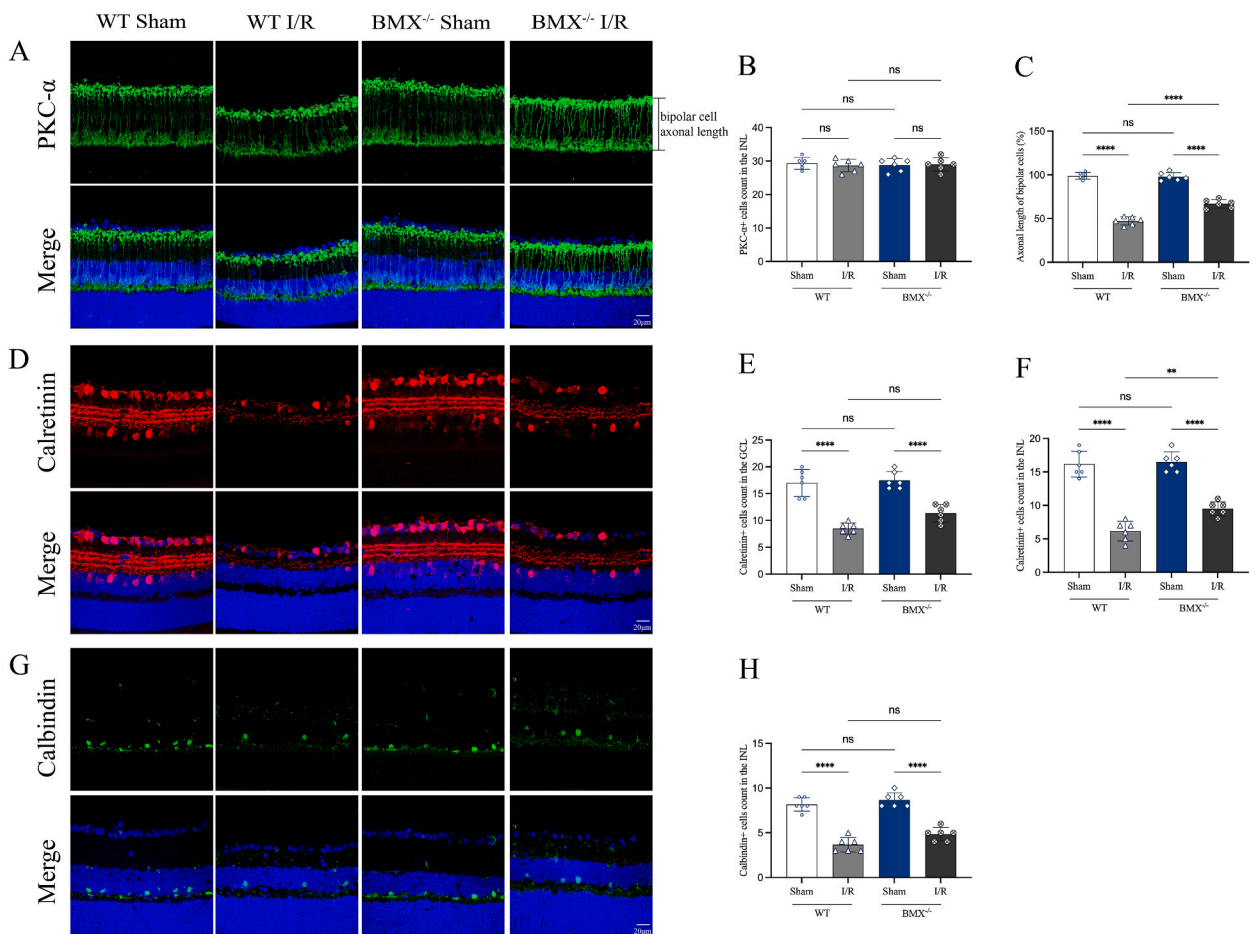


Fig. 3. $BMX^{-/-}$ alleviates the retinal neuronal damage following I/R injury. (A, D, G) Representative immunofluorescence images of PKC- α (green), calretinin (red), calbindin (green), and DAPI (blue) in WT + sham group, WT + I/R group, $BMX^{-/-}$ + sham group, and $BMX^{-/-}$ + I/R group, respectively. Scale bars = 20 μ m. (B–C) Quantification of PKC- α -positive rod bipolar cells in the INL and axonal length of PKC- α -positive rod bipolar cells. $n = 6$. (E–F) Measurement of calretinin-positive amacrine cells within the GCL and INL. $n = 6$. (H) Measurement of calbindin-positive horizontal cells within the INL. $n = 6$. Data are subsequent as mean \pm SEM and statistical significance has been identified utilizing One-way ANOVA subsequent by Tukey's Honest Significant Difference test. BMX, Bone marrow tyrosine kinase on chromosome X; I/R, ischemia/reperfusion; WT, wild type; GCL, ganglion cell layer; INL, inner nuclear layer; ns, nonsignificant; In this context, the symbols *, **, ***, and **** correspond to P-values that are below the thresholds of 0.05, 0.01, 0.001, and 0.0001, respectively. (For interpretation of the references to color in this figure legend, the reader is referred to the Web version of this article.)

3.3. *BMX*^{-/-} ameliorated damage to retinal structures after I/R injury

For a complete assessment of the alterations in retinal structure subsequent to retinal I/R injury, we conducted an analysis of the histomorphological changes in retinal tissue utilizing H&E staining, specifically focusing on a 7-day period following I/R injury. Within the context of WT mice, the inner retina's thickness, encompassing NFL/GCL, IPL, INL, OPL, and ONL, exhibited significant thinning following I/R injury contrasted with the WT + sham group (Fig. 2A–G). However, *BMX*^{-/-} mice displayed a partial rescue of retinal tissue loss following I/R injury (Fig. 2A–G). Furthermore, we conducted an assessment of the retinal structural alterations in mice through the utilization of SD-OCT at the in vivo level. The examination using SD-OCT unveiled a significant reduction in RNFL, GCC, and total retinal thickness within WT mice on the seventh day subsequent to I/R injury (Fig. 2H–K). In contrast, *BMX*^{-/-} mice exhibited the ability to salvage a portion of the retinal tissue subsequent to I/R injury (Fig. 2H–K). In light of the aforementioned experimental findings, we propose that *BMX* knockdown possesses the potential to alleviate the retina's structural impairment

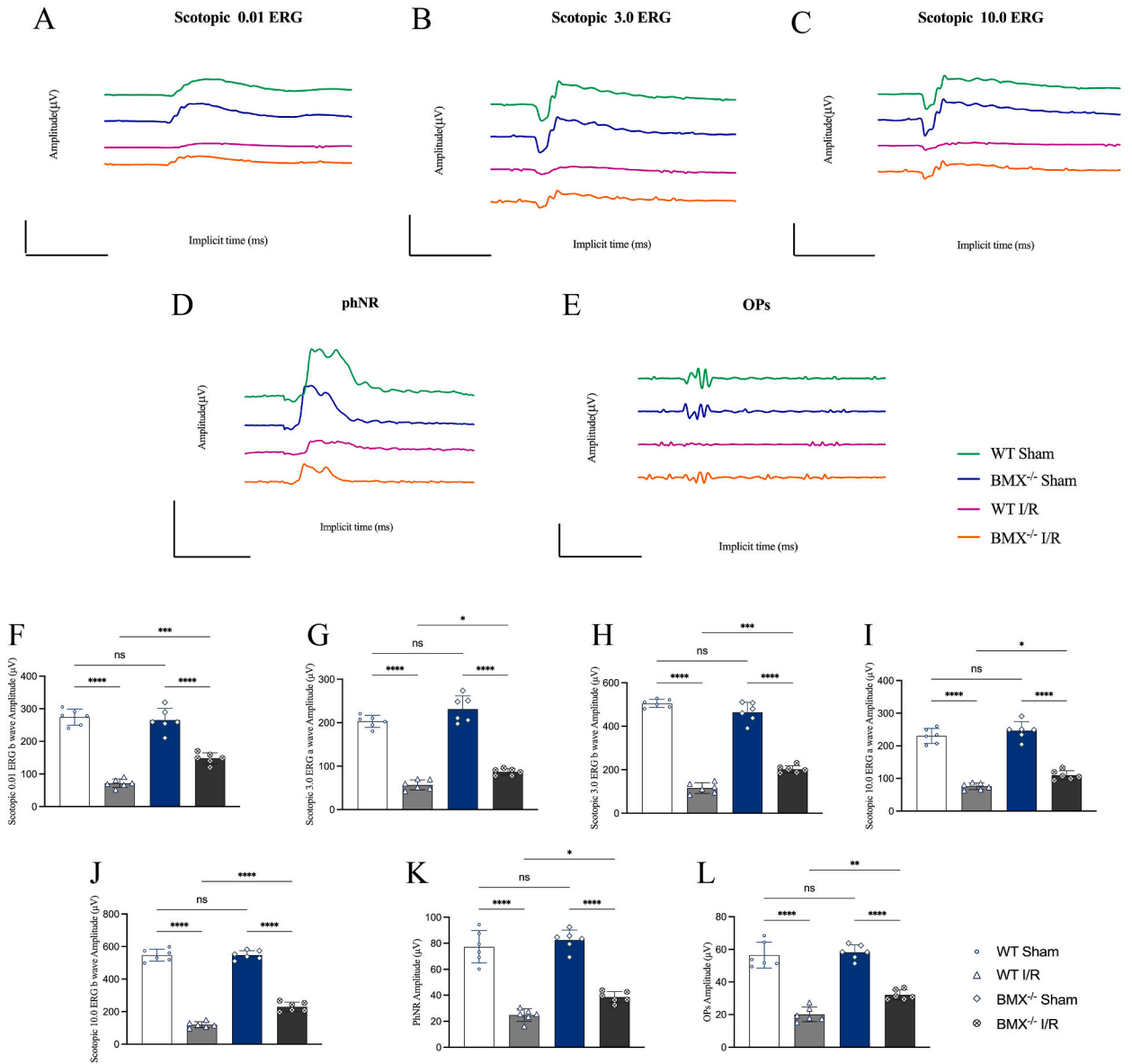


Fig. 4. *BMX*^{-/-} alleviated visual impairment after I/R injury. (A–E) Representative waveforms of the scotopic ERG, PhNR, and OPs in WT + sham group, WT + I/R group, *BMX*^{-/-} + sham group, and *BMX*^{-/-} + I/R group, respectively. (F–L) Quantification of the capacities of b-wave, a-wave, PhNR, and OPs. n = 6. Data are presented as mean ± SEM, and statistical significance has been identified utilizing One-way ANOVA subsequent by Tukey's Honest Significant Difference test. *BMX*, Bone marrow tyrosine kinase on chromosome X; I/R, ischemia/reperfusion; WT, wild type; ERG, electroretinography; PhNR, photopic negative response; ns, nonsignificant; In this context, the symbols *, **, ***, and **** correspond to P-values that are below the thresholds of 0.05, 0.01, 0.001, and 0.0001, respectively.

following I/R injury.

3.4. *BMX*^{-/-} alleviated retinal neuronal injury subsequent to I/R injury

In order to assess the extent of neuronal impairment within the inner retinal layers, we conducted an analysis on bipolar cells (specifically marked with PKC- α), amacrine cells (specifically marked with calretinin), and horizontal cells (specifically marked with calbindin) through the application of immunofluorescence staining. Despite no significant variation within the quantity of PKC- α -positive cells across the groups, our investigation revealed notable distinctions through the assessment of bipolar cell axonal length. Specifically, a statistically significant decrease has been detected within bipolar cell axonal length in WT mice at day 7 following I/R injury, in contrast to *BMX*^{-/-} mice, which exhibited a capacity to mitigate the extent of shortened bipolar cell axons subsequent to I/R injury (Fig. 3A–C). Additionally, WT mice demonstrated a noteworthy decrease in the quantity of calretinin-positive cells in the GCL and INL layers of the retina after seven days of I/R injury, in contrast to *BMX*^{-/-} mice, which exhibited partial restoration of calretinin-positive cells within the INL while no significant impact within the GCL (Fig. 3D–F). The quantity of calbindin-positive cells experienced a notable and comparable decline subsequent to I/R injury; however, *BMX*^{-/-} mice failed to exhibit a reversal of this alteration (Fig. 3G and H). The above results suggest that *BMX* knockdown can effectively protect neurons within the inner retina following I/R injury, especially the bipolar cell’s axon lengths and amacrine cells across the INL layer.

3.5. *BMX*^{-/-} alleviated visual impairment following I/R injury

To assess the visual function of retinal neurons, we performed an analysis of the visual function in each group prior to and

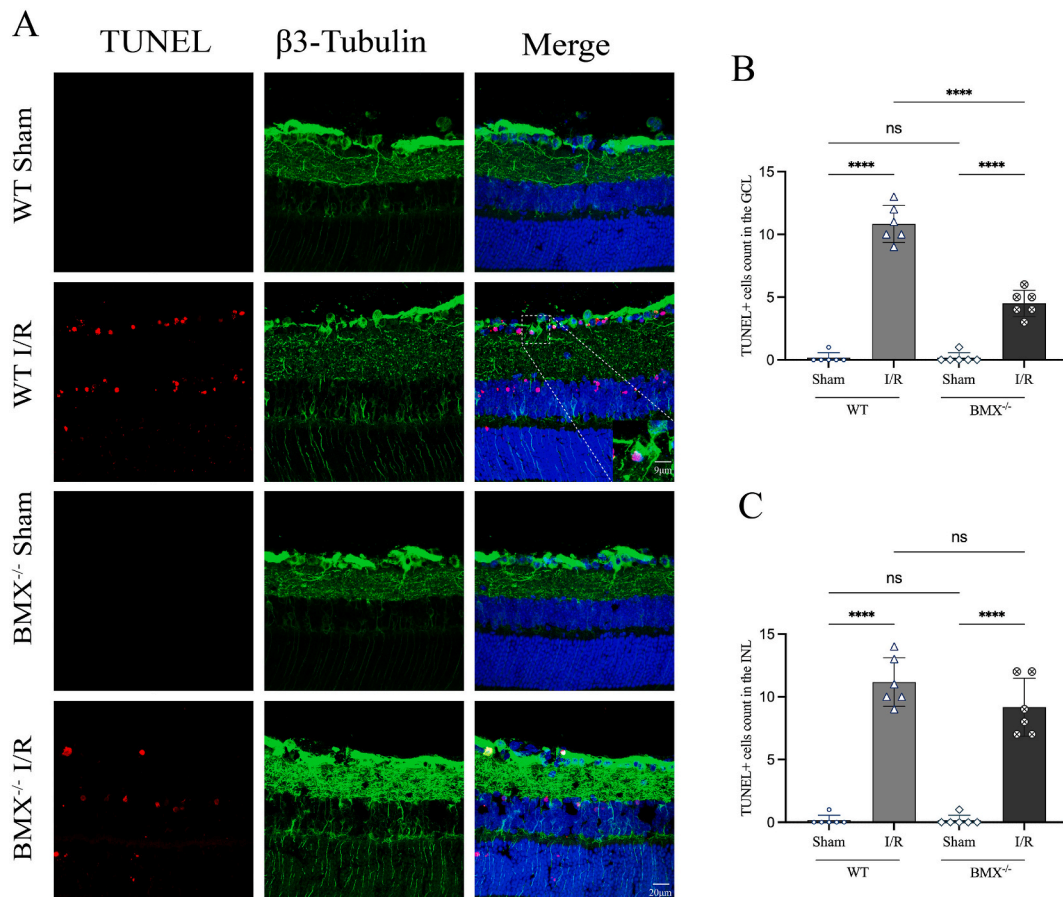


Fig. 5. *BMX*^{-/-} reduced RGCs apoptosis after I/R injury. (A) Representative immunofluorescence images of TUNEL (red), β 3-Tubulin (green), and DAPI (blue) in WT + sham group, WT + I/R group, *BMX*^{-/-} + sham group, and *BMX*^{-/-} + I/R group, respectively. Scale bars = 20 μ m. (B–C) Measurement of TUNEL-positive cells in the GCL and INL. n = 6. Data are presented as mean \pm SEM, and statistical significance has been identified utilizing One-way ANOVA subsequent by Tukey’s Honest Significant Difference test. *BMX*, Bone marrow tyrosine kinase on chromosome X; I/R, ischemia/reperfusion; WT, wild type; ns, nonsignificant; In this context, the symbols *, **, ***, and **** correspond to P-values that are below the thresholds of 0.05, 0.01, 0.001, and 0.0001, respectively. (For interpretation of the references to color in this figure legend, the reader is referred to the Web version of this article.)

subsequent I/R injury using ERG examination. Specifically, we examined the scotopic a-wave, b-wave, PhNR, and OPs, which serve as indicators of the functionality of RGCs, photoreceptors, bipolar cells, and amacrine cells, respectively. Our findings indicated that the extents of a-wave (Fig. 4B–C, G, and I), b-wave (Fig. 4A–C, F, H, and J), PhNR (Fig. 4D and K), and OPs (Fig. 4E and L) were significantly reduced in the WT + I/R group. Nevertheless, the BMX^{-/-} + I/R group showed a partial elevation in the extents of a-wave (Fig. 4B–C, G, and I), b-wave (Fig. 4A–C, F, H, and J), PhNR (Fig. 4D and K) and OPs (Fig. 4E and L) following I/R injury contrasted to the WT + I/R group. These results provided evidence that BMX^{-/-} can effectively alleviate visual function impairment in mice following I/R injury.

3.6. BMX^{-/-} rescued RGCs apoptosis after I/R injury

Apoptosis performs a critical function across the initiation of retinal impairment subsequent to I/R. To investigate the impact of BMX knockdown on apoptosis occurrence, we conducted TUNEL staining. Our findings revealed a notable rise within the quantity of TUNEL-positive cells across the GCL and INL layer of retina in WT + I/R group. Conversely, BMX^{-/-} + I/R group mice exhibited a statistically significant decrease in the quantity of TUNEL-positive cells within the GCL layers, whereas no significant difference has been detected within the INL layer (Fig. 5A–C). To acquire a more profound understanding of the localization of TUNEL-positive cells within the retina, we additionally observed the co-localization of TUNEL and the RGCs-specific marker β3-tubulin through immunofluorescence staining. These findings indicated that BMX^{-/-} considerably decreased the number of apoptotic cells within the retina GCL layers in mice following I/R and specifically inhibited RGCs apoptosis.

3.7. BMX^{-/-} inhibited the inflammatory response subsequent to I/R injury

The precise function of inflammatory responses within the progression of I/R is well-established, and retinal I/R injury induces glial

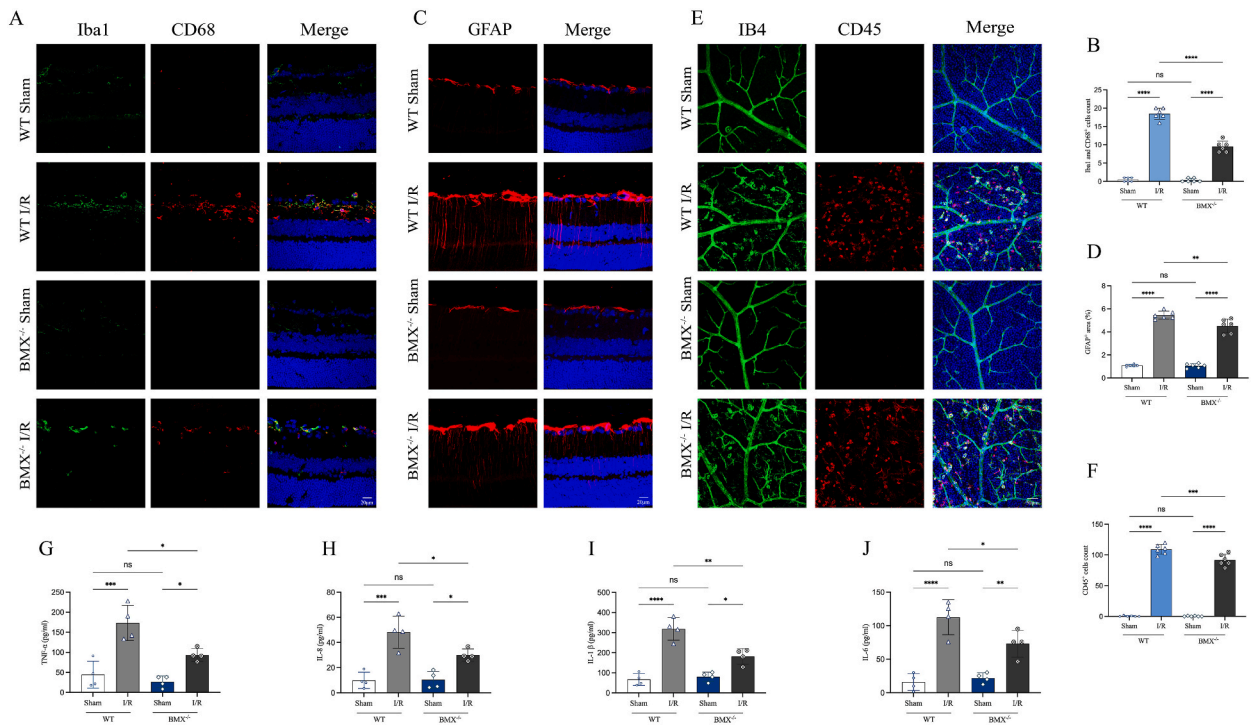


Fig. 6. BMX^{-/-} inhibited macrophage and astrocyte activation subsequent to I/R injury and reduced the inflammatory response surrounding retinal vessels. (A) Representative immunofluorescence images of Iba1 (green), CD68 (red), and DAPI (blue) in WT + sham group, WT + I/R group, BMX^{-/-} + sham group, and BMX^{-/-} + I/R group, respectively. Scale bars = 20 μm. (B) Measurement of Iba1- and CD68-positive activated microglia. n = 6. (C) Representative immunofluorescence images of GFAP (red) and DAPI (blue) in WT + sham group, WT + I/R group, BMX^{-/-} + sham group, and BMX^{-/-} + I/R group, respectively. Scale bars = 20 μm. (D) Measurement of GFAP-positive area. n = 6. (E) Representative immunofluorescence images of IB4 (green), CD45 (red), and DAPI (blue) in WT + sham group, WT + I/R group, BMX^{-/-} + sham group, and BMX^{-/-} + I/R group, respectively. Scale bars = 50 μm. (F) Measurement of CD45-positive leukocyte cells. n = 6. (G–J) Levels of the inflammatory factors TNF-α, IL-2, IL-1β, and IL-6 were determined by ELISA. n = 4. Data are presented as mean ± SEM, and statistical significance has been identified utilizing One-way ANOVA subsequent by Tukey’s Honest Significant Difference test. BMX, Bone marrow tyrosine kinase on chromosome X; I/R, ischemia/reperfusion; WT, wild type; ns, nonsignificant; In this context, the symbols *, **, ***, and **** correspond to P-values that are below the thresholds of 0.05, 0.01, 0.001, and 0.0001, respectively. (For interpretation of the references to color in this figure legend, the reader is referred to the Web version of this article.)

cell stimulation and heightened perivascular inflammation. For evaluating the impact of $BMX^{-/-}$ on the inflammatory response subsequent to retinal I/R injury, we conducted immunofluorescence staining for Iba1/CD68, GFAP, and CD45, which represent macrophages, astrocytes/Müller cells, and leukocytes, respectively. Moreover, the data presented in our study revealed a notable elevation in the presence of Iba1/CD68 (Fig. 6A and B), GFAP (Fig. 6C and D), and CD45-positive cells (Fig. 6E and F) within the WT + I/R group, contrasted with a significant decrease in these cell types within $BMX^{-/-}$ + I/R group mice (Fig. 6A–F). Furthermore, the inflammatory factors levels within the retina were assessed using ELISA, revealing a statistically significant elevation within the contexts of IL-8, IL-1 β , IL-6, and TNF- α expression levels within the WT + I/R group following I/R injury. However, the observed elevation was effectively mitigated by $BMX^{-/-}$ (Fig. 6G–J). These findings indicated that $BMX^{-/-}$ effectively inhibited the induction of macrophages and astrocytes/Müller cells, resulting in a reduction in the inflammatory infiltrate surrounding retinal vessels and a decrease in the release of inflammatory factors.

3.8. $BMX^{-/-}$ attenuated I/R injury of the Retina through suppressing the AKT/ERK/STAT3 signalling pathway

In order to investigate the mechanism whereby $BMX^{-/-}$ affects retinal I/R injury, we conducted an examination of the downstream factors regulated by BMX. The findings revealed that the WT + I/R group exhibited a notable increase within p-AKT, p-ERK, and p-STAT3 proteins expression levels following I/R injury, whereas BMX knockdown significantly decreased their expression (Fig. 7A–G). Additionally, it was observed that BMX knockdown did not have a significant impact on the levels of AKT, ERK, and STAT3 proteins (Fig. 7A–G). These outcomes suggested that $BMX^{-/-}$ mitigates I/R injury of the retina by suppressing the phosphorylation of AKT/ERK/STAT3 pathway.

4. Discussion

The loss of RGCs and irreversible impairment of retinal composition and activity are resulted from retinal I/R injury, ultimately leading to blindness. Consequently, the identification of effective neuroprotective targets and drugs continues to be a crucial and formidable task within the management of retinal I/R injury. The findings of our research demonstrate that the knockout of BMX exhibits protective characteristics contra retinal I/R injury. This is proved through the observation that $BMX^{-/-}$ effectively mitigated the detrimental influence of I/R injury on retinal tissue structure and visual function in mice. Moreover, $BMX^{-/-}$ demonstrated efficacy in reducing apoptosis and suppressing inflammatory responses. Furthermore, our results indicate that the attenuation of retinal I/R damage by $BMX^{-/-}$ is partially mediated through the inhibition of phosphorylation within the AKT/ERK/STAT3 signaling pathway. Meanwhile, in light of the fact that the absence of BMX does not exert any influence on the typical structure and functionality of the retina, it is plausible to consider inhibiting BMX as a prospective therapeutic approach for addressing retinal I/R injury. By doing so, it

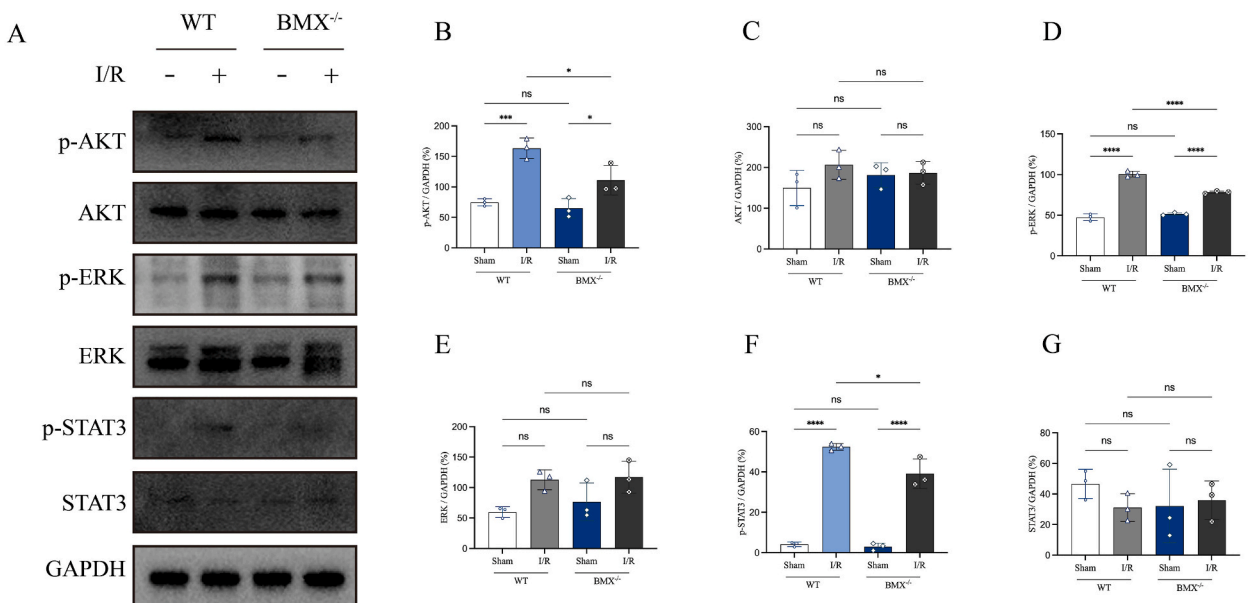


Fig. 7. Knockout of BMX attenuated retinal I/R damage by inhibiting the AKT/ERK/STAT3 signaling pathway. (A–G) Western blot and densitometry analyses of p-AKT, AKT, p-ERK, ERK, p-STAT3, and STAT3 expression in WT + sham group, WT + I/R group, $BMX^{-/-}$ + sham group, and $BMX^{-/-}$ + I/R group, respectively, with GAPDH utilized as a loading control. $n = 3$. Data are presented as mean \pm SEM, and statistical significance has been identified utilizing One-way ANOVA subsequent by Tukey's Honest Significant Difference test. BMX, Bone marrow tyrosine kinase on chromosome X; I/R, ischemia/reperfusion; WT, wild type; ns, nonsignificant; In this context, the symbols *, **, ***, and **** correspond to P-values that are below the thresholds of 0.05, 0.01, 0.001, and 0.0001, respectively.

may be possible to mitigate the decline in RGCs following retinal I/R injury, consequently resulting in an enhancement in visual activity.

BMX is a family member of a non-receptor tyrosine kinase Tec family and performs a pivotal function within numerous cellular pathways encompassing cell progression, survival, differentiation, growth signaling, cytokine signaling, and inflammation [10, 16–20]. The findings of the current investigation revealed a significant upregulation within BMX protein expression across the retinal tissue of WT mice following I/R injury. This observation was according to the immunofluorescence staining findings, which also demonstrated a similar trend. Notably, these results are in line with a prior investigation that documented augmented expression and strong phosphorylation of BMX in cardiac endothelial cells within an Ang II-induced cardiac hypertrophy model [21]. Additionally, Chen et al. observed a similar trend in primary cortical neurons following cerebral ischemic injury and demonstrated that inhibiting BMX activity protected against neurodegeneration in the ischemic brain [12]. BMX performs an essential function in regulating the function of various tyrosine kinases by facilitating phosphorylation at the pYpY site within the kinase domain of multi-receptor tyrosine kinases [22]. As a result, this regulatory mechanism has the potential to exert a widespread impact on the activity of multiple tyrosine kinases. Based on our research findings, we propose the hypothesis that BMX might be included within retinal I/R injury medication through the modulation of tyrosine kinase phosphorylation levels. Furthermore, we suggest that BMX could be a crucial target for intervention in retinal I/R injury management.

Retinal I/R injury might lead to a range of severe outcomes, primarily distinguished by the depletion of retinal neuron cells, resulting in retinal atrophy and thinning, along with damage to visual function [13,23–25]. Our findings align closely with prior research. Subsequent to I/R injury within WT mice, immunofluorescence staining analysis revealed a notable reduction within the count of RGCs, horizontal cells, and amacrine cells. However, the knockout of BMX can partially mitigate the detrimental effects of I/R injury on RGCs and INL layer amacrine cells. Significantly, our study yielded consistent results with Bai et al. [13], given the absence of any alteration in the quantity of rod bipolar cells. Nevertheless, our investigation additionally encompassed the assessment of bipolar cell axonal length, revealing a noteworthy reduction subsequent to the occurrence of I/R injury. Rod bipolar cells are primarily responsible for the processing and transmission of signals from photoreceptor cells to RGCs through chemical synapses, performing a critical function within the modulation and transmission of visual information [26]. Our findings revealed a substantial decrease within the capacity of ERG scotopic b-wave, indicating severe impairment of rod bipolar cell function subsequent to I/R injury. As for the shortening of rod bipolar cells' axon length, we speculated that it might be due to the thinning of the entire inner retina, potentially leading to the observed reduction in length. For retinal histomorphometry, our findings indicated a statistically significant reduction within the total thickness of the retina, and in the thickness of NFL/GCL, IPL, INL, OPL, RNFL, and GCC following I/R injury, according to H&E staining and SD-OCT techniques. Additionally, our examination using ERG demonstrated a statistically significant reduction within the capacities of PhNR, scotopic a-wave, and OPs following I/R injury, suggesting impaired functionality of RGCs, photoreceptors, and amacrine cells. This study presents empirical evidence demonstrating that the knockout of BMX effectively mitigates histological damage and visual function impairment after the incidence of retinal I/R injury.

Apoptosis was recognized as a prominent mechanism contributing to RGCs loss subsequent to retinal I/R injury, as evidenced by multiple studies [27–29]. The TUNEL assay, a well-established technique, has been extensively employed to detect and quantify DNA fragmentation and apoptosis induced by diverse forms of damage, including hypoxia [30,31]. The findings of our study indicated a noteworthy elevation in the quantity of TUNEL-positive cells in WT mice following I/R injury, particularly within the retina INL and GCL, aligning with previous research outcomes [27]. Conversely, the $BMX^{-/-}$ + I/R group exhibited a significantly lower count of TUNEL-positive cells contrasted with the WT + I/R group. Consequently, the outcomes of this investigation propose that BMX knockdown can effectively mitigate apoptosis in the retina.

Inflammation is a crucial defense mechanism orchestrated by the host immune system and performs a significant function in the physiological functioning of the organism [32–34]. The retinal tissue possesses an immune system that exhibits high sensitivity, with microglia serving as the resident immune cells responsible for detecting and transmitting immune signals within the retina [35,36]. In instances of pathological conditions, microglia become activated and swiftly relocate to the outer retina, subsequently releasing cytokines and chemokines that facilitate neuronal apoptosis in the retinal region [37,38]. Our investigation results revealed that after I/R injury to the retina, microglia exhibited significant activation and migration towards the outer retina, particularly in the GCL. Additionally, we detected a substantial elevation within the inflammatory factors' expression levels, involving IL-8, IL-1 β , IL-6, and TNF- α within the retina. Notably, the knockout of BMX led to a substantial decrease in microglia activation and a downregulation of inflammatory factor levels. Furthermore, the main neuroglia of the retina are Müller cells, astrocytes, and microglia, which play crucial roles in maintaining tissue homeostasis by interacting with neurons, immune cells, and blood vessels [39]. Our research also demonstrated that following I/R injury, there is a notable induction of astrocytes/Müller cells, combined with a substantial infiltration of leukocytes surrounding retinal blood vessels. Notably, the inhibition of BMX expression significantly suppressed the induction of astrocytes/Müller cells and mitigated the inflammatory infiltration surrounding retinal vessels. Based on the aforementioned findings, it is postulated that the knockdown of BMX may effectively mitigate the inflammatory response following the retinal I/R injury occurrence, thereby diminishing the apoptosis of RGCs and ultimately manifesting a neuroprotective impact. However, the research presented in this study does not provide sufficient evidence to establish a direct correlation between BMX-induced inflammation and RGCs apoptosis following glial cell activation. Therefore, further investigation is imperative to elucidate the potential regulatory mechanisms governing this association.

The significant involvement of BMX in cytokine signaling and inflammation was extensively acknowledged [8,10]; nevertheless, the precise molecular mechanisms through which it contributes to retinal I/R injury remain unresolved. The gene STAT3 is widely recognized as a significant contributor to stress response, cell survival, and inflammation [40]. Research has demonstrated that the activation of STAT3 performs a pivotal function within the inflammatory response stimulated via elevated glucose levels in retinal

endothelial cells. Furthermore, inhibiting or reducing the expression of STAT3 has been found to decrease the levels of TNF- α expression and pERK phosphorylation in retinal endothelial cells [41,42]. Additionally, studies have revealed that BMX can effectively activate STAT3, thereby exhibiting anti-tumor and anti-drug resistance properties [43–45]. Furthermore, we discovered that the AKT and ERK pathway performs a crucial function in modulating the inflammatory response observed in retinopathy resulting from I/R injury, hyperglycemia, or LPS stimulation [28,46–49]. Prior research has indicated that the levels of p-AKT, particularly p-AKT1, and the phosphorylation levels of its principal downstream transcription factors, play a role in the onset and advancement of inflammation following liver ischemia-reperfusion injury [50,51]. For investigating the underlying molecular mechanisms through which the knockout of BMX mitigates the inflammatory response and neurological impairment stimulated via retinal I/R injury, we conducted an examination of the AKT/ERK/STAT3 signaling pathway. The findings of our investigation indicate a statistically significant elevation in the expression of phosphorylated AKT, ERK, and STAT3 proteins subsequent to retinal I/R injury incidence. Nevertheless, the knockout of BMX resulted in a notable reduction in the levels of phosphorylated AKT, ERK, and STAT3 proteins. Hence, it is proposed that the knockout of BMX gene expression mitigates the inflammatory reaction and neural impairment subsequent to retinal I/R injury, partly through modulation of the phosphorylation status of AKT/ERK/STAT3 signaling cascade.

5. Conclusion

In conclusion, our study provided evidence that the knockout of BMX can induce anti-apoptotic and anti-inflammatory effects by decreasing the phosphorylation level of downstream AKT, ERK, and STAT3 pathways. Within the context of the retinal I/R injury mouse model, this protected retinal structure and function. Consequently, targeting BMX inhibition may be an important management technique subsequent to the incidence of retinal I/R injury, warranting further investigation in clinical studies.

Funding

This work was supported by the Guangxi Clinical Ophthalmic Research Center (No. GuikeAD19245193), the Natural Science Foundation of Guangxi Zhuang Autonomous Region (No.2021GXNSFAA220005, 2020GXNSFBA159015, No.2023GXNSFAA026074), Guangxi Science and Technology Base and Talent Special Fund (GUI KEAD20297030), the National Natural Science Foundation of China (No.82060179, 82070982, 82101096).

Ethics statement

This study was reviewed and approved by Animal Experiment Ethics Committee of Guangxi Medical University, with the approval number: 202209005.

Data availability statement

The datasets used and/or analyzed during the current study available from the corresponding author on reasonable request.

CRedit authorship contribution statement

Guangyi Huang: Writing – original draft, Data curation. **Shaoyang Zhang:** Formal analysis. **Jing Liao:** Formal analysis, Data curation. **Yuanjun Qin:** Data curation, Conceptualization. **Yiyi Hong:** Validation, Data curation. **Qi Chen:** Validation, Formal analysis. **Yunru Lin:** Validation, Formal analysis. **Yue Li:** Formal analysis, Data curation. **Lin Lan:** Validation, Data curation. **Wen Hu:** Formal analysis, Data curation. **Kongqian Huang:** Validation, Data curation. **Fen Tang:** Validation, Supervision. **Ningning Tang:** Validation, Conceptualization. **Li Jiang:** Validation, Funding acquisition, Conceptualization. **Chaolan Shen:** Writing – review & editing, Data curation. **Ling Cui:** Project administration, Funding acquisition. **Haibin Zhong:** Funding acquisition, Conceptualization. **Min Li:** Funding acquisition, Conceptualization. **Peng Lu:** Formal analysis, Conceptualization. **Qinmeng Shu:** Conceptualization. **Yantao Wei:** Validation, Conceptualization. **Fan Xu:** Validation, Project administration, Conceptualization.

Declaration of competing interest

The authors declare that they have no known competing financial interests or personal relationships that could have appeared to influence the work reported in this paper.

Acknowledgements

None to report.

Appendix A. Supplementary data

Supplementary data to this article can be found online at <https://doi.org/10.1016/j.heliyon.2024.e27114>.

References

- [1] A. Pefanis, F.L. Ierino, J.M. Murphy, et al., Regulated necrosis in kidney ischemia-reperfusion injury, *Kidney Int.* 96 (2) (2019) 291–301.
- [2] T.F. Chen-Yoshikawa, Ischemia-reperfusion injury in lung Transplantation, *Cells* 10 (6) (2021).
- [3] Y. Liu, T. Lu, C. Zhang, et al., Activation of YAP attenuates hepatic damage and fibrosis in liver ischemia-reperfusion injury, *J. Hepatol.* 71 (4) (2019) 719–730.
- [4] S.F. Abcouwer, S. Shanmugam, A. Muthusamy, et al., Inflammatory resolution and vascular barrier restoration after retinal ischemia reperfusion injury, *J. Neuroinflammation* 18 (1) (2021) 186.
- [5] G. Neves, L. Lagnado, The retina, *Curr. Biol.* 9 (18) (1999) R674–R677.
- [6] N.J. Horwood, A.M. Urbaniak, L. Danks, Tec family kinases in inflammation and disease, *Int. Rev. Immunol.* 31 (2) (2012) 87–103.
- [7] B. Cenni, S. Gutmann, M. Gottar-Guillier, BMX and its role in inflammation, cardiovascular disease, and cancer, *Int. Rev. Immunol.* 31 (2) (2012) 166–173.
- [8] L. Qiu, F. Wang, S. Liu, et al., Current understanding of tyrosine kinase BMX in inflammation and its inhibitors, *Burns Trauma* 2 (3) (2014) 121–124.
- [9] C.D. Palmer, B.E. Mutch, S. Workman, et al., Bmx tyrosine kinase regulates TLR4-induced IL-6 production in human macrophages independently of p38 MAPK and NFκapp)B activity, *Blood* 111 (4) (2008) 1781–1788.
- [10] M. Gottar-Guillier, F. Dodeller, D. Huesken, et al., The tyrosine kinase BMX is an essential mediator of inflammatory arthritis in a kinase-independent manner, *J. Immunol.* 186 (10) (2011) 6014–6023.
- [11] F. Yang, M. Duan, F. Zheng, et al., Fas signaling in adipocytes promotes low-grade inflammation and lung metastasis of colorectal cancer through interaction with Bmx, *Cancer Lett.* 522 (2021) 93–104.
- [12] K.Y. Chen, C.C. Wu, C.F. Chang, et al., Suppression of Etk/Bmx protects against ischemic brain injury, *Cell Transplant.* 21 (1) (2012) 345–354.
- [13] X. Bai, D. Ye, Y. Shi, et al., Neuroprotection of SRT2104 in murine ischemia/reperfusion injury through the enhancement of sirt1-mediated deacetylation, *Invest. Ophthalmol. Vis. Sci.* 64 (4) (2023) 31.
- [14] D. Ye, Y. Xu, Y. Shi, et al., Anti-PANoptosis is involved in neuroprotective effects of melatonin in acute ocular hypertension model, *J. Pineal Res.* 73 (4) (2022) e12828.
- [15] W. Liu, Y. Ha, F. Xia, et al., Neuronal Epac1 mediates retinal neurodegeneration in mouse models of ocular hypertension, *J. Exp. Med.* 217 (4) (2020).
- [16] C.H. Chau, C.A. Clavijo, H.T. Deng, et al., Etk/Bmx mediates expression of stress-induced adaptive genes VEGF, PAI-1, and iNOS via multiple signaling cascades in different cell systems, *Am. J. Physiol. Cell Physiol.* 289 (2) (2005) C444–C454.
- [17] N. Ekman, E. Arighi, I. Rajantie, et al., The Bmx tyrosine kinase is activated by IL-3 and G-CSF in a PI-3K dependent manner, *Oncogene* 19 (36) (2000) 4151–4158.
- [18] C.H. Chau, K.Y. Chen, H.T. Deng, et al., Coordinating Etk/Bmx activation and VEGF upregulation to promote cell survival and proliferation, *Oncogene* 21 (57) (2002) 8817–8829.
- [19] L. Tamagnone, I. Lahtinen, T. Mustonen, et al., BMX, a novel nonreceptor tyrosine kinase gene of the BTK/ITK/TEC/TKX family located in chromosome Xp22.2, *Oncogene* 9 (12) (1994) 3683–3688.
- [20] Y. Qiu, H.J. Kung, Signaling network of the Btk family kinases, *Oncogene* 19 (49) (2000) 5651–5661.
- [21] T. Holopainen, M. Räsänen, A. Anisimov, et al., Endothelial Bmx tyrosine kinase activity is essential for myocardial hypertrophy and remodeling, *Proc. Natl. Acad. Sci. U. S. A.* 112 (42) (2015) 13063–13068.
- [22] S. Chen, X. Jiang, C.A. Gewinner, et al., Tyrosine kinase BMX phosphorylates phosphotyrosine-primed motif mediating the activation of multiple receptor tyrosine kinases, *Sci. Signal.* 6 (277) (2013) ra40.
- [23] H. Schmid, M. Renner, H.B. Dick, et al., Loss of inner retinal neurons after retinal ischemia in rats, *Invest. Ophthalmol. Vis. Sci.* 55 (4) (2014) 2777–2787.
- [24] Y. Mukaida, S. Machida, T. Masuda, et al., Correlation of retinal function with retinal histopathology following ischemia-reperfusion in rat eyes, *Curr. Eye Res.* 28 (6) (2004) 381–389.
- [25] W. Liu, F. Xia, Y. Ha, et al., Neuroprotective effects of HSF1 in retinal ischemia-reperfusion injury, *Invest. Ophthalmol. Vis. Sci.* 60 (4) (2019) 965–977.
- [26] U. Grünert, P.R. Martin, Rod bipolar cells in the macaque monkey retina: immunoreactivity and connectivity, *J. Neurosci.* 11 (9) (1991) 2742–2758.
- [27] N. Jiang, Z. Li, Z. Li, et al., Laquinimod exerts anti-inflammatory and antiapoptotic effects in retinal ischemia/reperfusion injury, *Int. Immunopharm.* 88 (2020) 106989.
- [28] A. Yu, S. Wang, Y. Xing, et al., 7,8-Dihydroxyflavone alleviates apoptosis and inflammation induced by retinal ischemia-reperfusion injury via activating TrkB/Akt/NF-κB signaling pathway, *Int. J. Med. Sci.* 19 (1) (2022) 13–24.
- [29] T.T. Lam, A.S. Abler, M.O. Tso, Apoptosis and caspases after ischemia-reperfusion injury in rat retina, *Invest. Ophthalmol. Vis. Sci.* 40 (5) (1999) 967–975.
- [30] C.L. Moore, A.V. Savenka, A.G. Basnakian, TUNEL assay: a powerful tool for kidney injury evaluation, *Int. J. Mol. Sci.* 22 (1) (2021).
- [31] P. Majtnerová, T. Rousar, An overview of apoptosis assays detecting DNA fragmentation, *Mol. Biol. Rep.* 45 (5) (2018) 1469–1478.
- [32] U. Weiss, Inflammation. *Nature* 454 (7203) (2008) 427.
- [33] C. Nathan, A. Ding, Nonresolving inflammation, *Cell* 140 (6) (2010) 871–882.
- [34] K.A. Wong, L.I. Benowitz, Retinal ganglion cell survival and axon regeneration after optic nerve injury: role of inflammation and other factors, *Int. J. Mol. Sci.* 23 (17) (2022).
- [35] I. Akhtar-Schäfer, L. Wang, T.U. Krohne, et al., Modulation of three key innate immune pathways for the most common retinal degenerative diseases, *EMBO Mol. Med.* 10 (10) (2018).
- [36] H. Kettenmann, U.K. Hanisch, M. Noda, et al., Physiology of microglia, *Physiol. Rev.* 91 (2) (2011) 461–553.
- [37] L. Du, Y. Zhang, Y. Chen, et al., Role of microglia in neurological disorders and their potentials as a therapeutic target, *Mol. Neurobiol.* 54 (10) (2017) 7567–7584.
- [38] G. Rathnasamy, W.S. Foulds, E.A. Ling, et al., Retinal microglia - a key player in healthy and diseased retina, *Prog. Neurobiol.* 173 (2019) 18–40.
- [39] E. Vecino, F.D. Rodriguez, N. Ruzafa, et al., Glia-neuron interactions in the mammalian retina, *Prog. Retin. Eye Res.* 51 (2016) 1–40.
- [40] H. Yu, D. Pardoll, R. Jove, STATs in cancer inflammation and immunity: a leading role for STAT3, *Nat. Rev. Cancer* 9 (11) (2009) 798–809.
- [41] Y. Chen, J.J. Wang, J. Li, et al., Activating transcription factor 4 mediates hyperglycaemia-induced endothelial inflammation and retinal vascular leakage through activation of STAT3 in a mouse model of type 1 diabetes, *Diabetologia* 55 (9) (2012) 2533–2545.
- [42] K.M. Cui, Z.P. Hu, Y.L. Wang, MG53 represses high glucose-induced inflammation and angiogenesis in human retinal endothelial cells by repressing the EGR1/STAT3 axis, *Immunopharmacol. Immunotoxicol.* 44 (4) (2022) 484–491.
- [43] O.A. Guryanova, Q. Wu, L. Cheng, et al., Nonreceptor tyrosine kinase BMX maintains self-renewal and tumorigenic potential of glioblastoma stem cells by activating STAT3, *Cancer Cell* 19 (4) (2011) 498–511.
- [44] X.F. Xu, J.J. Wang, L. Ding, et al., Suppression of BMX-ARHGAP fusion gene inhibits epithelial-mesenchymal transition in gastric cancer cells via RhoA-mediated blockade of JAK/STAT axis, *J. Cell. Biochem.* 120 (1) (2019) 439–451.
- [45] Y. Shi, O.A. Guryanova, W. Zhou, et al., Ibrutinib inactivates BMX-STAT3 in glioma stem cells to impair malignant growth and radioresistance, *Sci. Transl. Med.* 10 (443) (2018).
- [46] J. Yue, X. Zhao, GPR174 suppression attenuates retinopathy in angiotensin II (Ang II)-treated mice by reducing inflammation via PI3K/AKT signaling, *Biomed. Pharmacother.* 122 (2020) 109701.
- [47] R. Janani, R.E. Anitha, P. Divya, et al., Astaxanthin ameliorates hyperglycemia induced inflammation via PI3K/Akt-NF-κB signaling in ARPE-19 cells and diabetic rat retina, *Eur. J. Pharmacol.* 926 (2022) 174979.
- [48] S.H. Paeng, W.S. Park, W.K. Jung, et al., YCG063 inhibits *Pseudomonas aeruginosa* LPS-induced inflammation in human retinal pigment epithelial cells through the TLR2-mediated AKT/NF-κB pathway and ROS-independent pathways, *Int. J. Mol. Med.* 36 (3) (2015) 808–816.

- [49] F. Lazzara, A. Fidilio, C.B.M. Platania, et al., Aflibercept regulates retinal inflammation elicited by high glucose via the PIGF/ERK pathway, *Biochem. Pharmacol.* 168 (2019) 341–351.
- [50] Z. Huang, T. Mou, Y. Luo, et al., Inhibition of miR-450b-5p ameliorates hepatic ischemia/reperfusion injury via targeting CRYAB, *Cell Death Dis.* 11 (6) (2020) 455.
- [51] J.H. Li, J.J. Jia, N. He, et al., Exosome is involved in liver graft protection after remote ischemia reperfusion conditioning, *Hepatobiliary Pancreat. Dis. Int.* 22 (5) (2023) 498–503.